China Geology 7 (2024) 264–276

China Geology

Journal homepage: http://chinageology.cgs.cn
https://www.sciencedirect.com/journal/china-geology

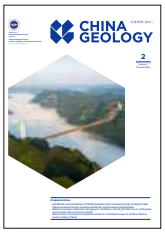

Runout prediction of potential landslides based on the multi-source data collaboration analysis on historical cases

Jun Sun[a], Yu Zhuang[b], Ai-guo Xing[b,*]

[a] *Guizhou Geology and Mineral Engineering Construction Co., Ltd, Guiyang* 550000, *China*
[b] *State Key Laboratory of Ocean Engineering, Shanghai Jiao Tong University, Shanghai* 200240, *China*

ARTICLE INFO

Article history:
Received 27 November 2023
Received in revised form 21 December 2023
Accepted 18 March 2024
Available online 17 April 2024

Keywords:
Landslide runout prediction
Drone survey
Multi-source data collaboration
DAN3D numerical modeling
Jianshanying landslide
Guizhou Province
Geological hazards survey engineering

ABSTRACT

Long runout landslides involve a massive amount of energy and can be extremely hazardous owing to their long movement distance, high mobility and strong destructive power. Numerical methods have been widely used to predict the landslide runout but a fundamental problem remained is how to determine the reliable numerical parameters. This study proposes a framework to predict the runout of potential landslides through multi-source data collaboration and numerical analysis of historical landslide events. Specifically, for the historical landslide cases, the landslide-induced seismic signal, geophysical surveys, and possible *in-situ* drone/phone videos (multi-source data collaboration) can validate the numerical results in terms of landslide dynamics and deposit features and help calibrate the numerical (rheological) parameters. Subsequently, the calibrated numerical parameters can be used to numerically predict the runout of potential landslides in the region with a similar geological setting to the recorded events. Application of the runout prediction approach to the 2020 Jiashanying landslide in Guizhou, China gives reasonable results in comparison to the field observations. The numerical parameters are determined from the multi-source data collaboration analysis of a historical case in the region (2019 Shuicheng landslide). The proposed framework for landslide runout prediction can be of great utility for landslide risk assessment and disaster reduction in mountainous regions worldwide.

1. Introduction

Long-runout landslides are among the most spectacular and catastrophic geologic processes. They are characterized by their large volume, high mobility, and long movement distance, causing mass casualties and economic loss worldwide (Geertsema M et al., 2006; Johnson BC and Campbell CS, 2017; Zhuang Y et al., 2019). Close attention is increasingly being paid to the risk assessment of long runout landslides, which aids the mitigation and prevention of potential landslide disasters (Miao T et al., 2001). The landslide risk assessment comprises two main questions: The location of landslide occurrence and the resulting consequences. For the first question, much effort has been made through the in-situ investigation, monitoring, and numerical methods. The monitoring techniques for the landslide deformation, representative by the interferometric synthetic aperture radar (InSAR) (Chen LQ et al., 2021; Novellino A et al., 2021), combined with the field investigation provide valuable information to identify the landslide location (Xu L et al., 2012). Furthermore, numerical methods (e.g., finite element method and limit equilibrium methods) (Morrison IM and Greenwood JR, 1989; Ishii Y et al., 2012; Zhuang Y et al., 2022) and borehole/geophysical surveys greatly help to determine the slope stability and potential sliding surface (McCann DM and Forster A, 1990; Yalcinkaya E et al., 2016).

Considering the severe consequences of long-runout landslides, it is essential to predict the landslide runout behaviors, especially their movement distance. The methods of predicting movement distance can be roughly grouped into empirical approaches, theoretical methods, and numerical modeling. The empirical approach is to establish the relationship model between sliding distance and impact

First author: *E-mail address*: 172129101@qq.com (Jun Sun).

* Corresponding author: *E-mail address*: xingaiguo@sjtu.edu.cn (Ai-guo Xing).

Literary editor: Xi-jie Chen
doi:10.31035/cg2023138
2096-5192/© 2024 China Geology Editorial Office.

factors through mathematical statistics, which is developed by reference to actual landslide data (e.g., Hunter G and Fell R, 2003; Fan XM et al., 2014). For the theoretical models, equations are proposed based on the energy principle and can briefly describe the landslide dynamics (e.g., Scheidegger AE, 1973; Shi C et al., 2013). Numerical modeling is primarily categorized into continuum-based methods and discrete numerical methods, and can provide good performance in simulating the whole landslide movement process and dynamic characteristics (Miao T et al., 2001).

The empirical and theoretical approaches have the advantages of simplicity and rapid assessment (e.g., the Heim' s ratio), but are limited by the accuracy of prediction results. The landslide movement is a complex process controlled by many factors (Tomás R et al., 2017). Except for the widely considered factors that are involved in the above two approaches, such as landslide volume, slope angle, and fall height, micro-topography also plays an essential role in the landslide movement. For instance, in the 2017 Nayong avalanche (Luo H et al., 2021) and the 2019 Shuicheng avalanche (Zhuang Y et al., 2021) in Guizhou, China, the ridge located in the travel path deflected the sliding mass and then caused mass casualties. Such an impact is hardly involved in a simple empirical or theoretical model to predict the landslide movement.

Numerical models based on the continuum (e.g., DAN-W, DAN3D, and RAMMS) (Hungr O and McDougall S, 2009; Christen M et al., 2010; Frank F et al., 2015; Zhuang Y et al., 2023a) and discrete (e.g., PFC, EDEM, and Matdem) (Itasca, Consulting Group, 2008; Thompson N et al., 2009; Liu C et al., 2013; DEM Solutions Ltd, 2019) mechanics have been favored in predicting the complex motion of landslide masses. Up to now, although the effectiveness of these models has been validated through the back-analysis of recorded landslides, successful prediction of landslide movement has been rarely reported. A fundamental problem has remained about the determination of numerical parameters. Back-analysis of case histories is essential to improve forecasting accuracy by providing parameters specific to similar types of landslides for use in predicting the runout distance. However, the parameters are not convincing if only the simulated travel path and deposit shape are consistent with the actual event (Zhuang Y et al., 2021). Several groups of parameters are commonly determined in such a condition. As pointed out by Storm A (2006), proposing reliable models and parameters for landslide movement modeling needs to account for the topographical and depositional features, and the observable phenomena should be regarded as constraints to validate the model. Therefore, extra efforts need to be paid to the dynamic behaviors and deposit characteristics of the events.

The landslide seismology, in-situ videos, and geophysical surveys have been confirmed to provide the opportunity for model validation. The seismic signal results from the landslide can be converted into a time series recording of the event (Ekström G and Stark CP, 2013; Iverson RM et al., 2015), and its combined contribution with in-situ videos from drones/phones can provide insights into the landslide dynamics (e.g., landslide duration, velocity, and runout distance) (He K et al., 2018; Zhu YQ et al., 2019). Furthermore, geophysical surveys (magnetic method, seismic method, and electrical method) have been widely used to identify the subsurface characteristics of landslides and provide data to determine the deposit distribution (Perrone A et al., 2014; Bellanova J et al., 2018). These multi-source data collaboration analysis results can validate the numerical results of historical events in terms of landslide dynamics and deposit characteristics, and greatly improve the accuracy of numerical parameters. The determined parameters will help the runout prediction of potential landslides in the region with a similar geological setting to the recorded events.

In this study, the authors first described the principle of predicting the potential landslide runout based on the multi-source data collaboration analysis on historical cases. Subsequently, this paper summarized our previous research on the 2019 Shuicheng landslide in Guizhou, China, providing insights into how to investigate the dynamics of historical landslides based on numerical modeling and multi-source data collaboration. The 2020 Jianshanying landslide, which is located near the Shuicheng landslide and has a similar geological setting, was then selected as a case study to conduct the runout distance prediction. The work in this study is expected to provide an applicable framework and new insights into the prediction of long-runout landslide travel distance.

2. Method for landslide runout prediction

Long runout landslides occur mostly in mountainous regions with the properties of suddenness and high mobility. Their impact properties are hardly observable, and monitoring equipment can get damaged because of the strong destructive power (Johnson BC and Campbell CS, 2017). Therefore, although many numerical methods have been established for landslide dynamics modeling, a fundamental question remained is how to determine the reliable numerical parameters because direct observation data are rarely available for model validation. In this study, the key of the method for landslide runout prediction is to first determine the accurate numerical parameters of historical landslide events through the combination of numerical modeling and multi-source data collaboration analysis. Subsequently, the calibrated numerical parameters are utilized for the runout prediction of potential landslides that have a similar geological setting to the recorded events.

In this study, the landslide movements are modeled by the DAN3D model. The multi-source data collaboration analysis includes the analysis of the landslide-induced seismic signal, the electrical resistivity tomography (ERT) method and the possible captured drone video. The landslide-induced seismic signal and captured drone video can capture the dynamic characteristics of recorded events, and the electrical resistivity tomography (ERT) method can help determine the deposit

features. These data can validate the modeling results of historical cases and calibrate the numerical parameters. A detailed description of multi-source data collaboration analysis and the DAN3D model are presented below. It is worth noting that the method proposed in this study is a framework. Thus, any other approaches to obtain the landslide properties and calibrate the rheological parameters can be incorporated.

2.1. Landslide seismology analysis

Large landslides can generate seismic waves strong enough to be captured by local seismic stations. These seismic data record the entire landslide process and could provide insights into the landslide dynamics. Arias intensity (I_A) can be used in seismology to describe the energy variation during the landslide motion. This index characterizes the duration of the landslide impact and erosion stages, and its expression is as follows:

$$I_A = \frac{\pi}{2g}\int_0^{T_d} a^2(t)\,dt \tag{1}$$

where $a(t)$ is the acceleration of the seismic signal, T_d is the signal duration, and g is the gravitational acceleration.

Further time-frequency analysis can help analyze the landslide dynamics through the Hibert transform (Hibert C et al., 2014). This process calculates the instantaneous frequencies and draws the amplitude-time-frequency spectrum of the landslide-induced seismic signal, which will greatly contribute to the investigation of landslide movement process.

The kinematic characteristic analysis can be conducted to analyze the landslide velocity and movement distance based on the interaction principle between sliding mass and the crust. When the landslide occurs, the displacement information recorded by the seismic station (U) can be expressed as the convolution of the crustal force-time function with the Green's function (G) (Stein S and Wysession M, 2003):

$$U(t) = F_e(t) * G(t) \tag{2}$$

where $F_e(t)$ refers to the force-time function, and can be determined through a discrete wave number Green's function. Subsequently, the landslide velocity and displacement can be obtained by integration when the crustal force-time function is calculated.

2.2. Electrical resistivity tomography

The ERT method is an electrical-based method to elucidate the resistivity contrast between materials and has been widely used for the landslide investigation. It can image the subsurface characteristics of landslide profiles according to electrical resistivity distribution and help estimate the deposit distribution. Resistivity measurements are conducted by inputting currents (I) into the subsoil and measuring the potential drop (ΔV) between electrodes (Sharma PS, 1997). The apparent resistivity (ρ_a) of subsurface soil is calculated using the Ohm's law:

$$\rho_a = K\frac{\Delta V}{I} \tag{3}$$

where K is the geometric factor relating to the configuration of electrodes, I is the current, and ΔV is the potential difference.

Various arrays can be used for the ERT measurement, and their advantages and limitations have been fully discussed (Furman A et al., 2003; Martorana R et al., 2017). Among the arrays, the Wenner array has been proved to be a robust quality array and is suitable for the subsurface investigation of a landslide (Rezaei S et al., 2019; Szczygieł J et al., 2019). After the in-situ measurement, the measured apparent resistivity can be inverted using the software RES-2Dinv to derive the electrical resistivity tomography. The RES-2Dinv software is one of the most common inversion algorithms, which calculates the actual resistivity values based on the smoothness-constrained least-squares method (Loke MH and Barker RD, 1996). More details regarding ERT measurement and inversion methods are presented in Zhuang Y et al. (2021). The combination of Wenner array and RES-2Dinv software is recommended for the measurement of landslide deposit distribution.

2.3. Dan3D model

The dynamic model DAN3D is a continuum-based method capable of simulating the entire landslide movement across a real 3D topography (McDougall S and Hungr O, 2005; Hungr O et al., 2005). The model is established based on the smoothed particle hydrodynamics (SPH) method and treats the complex landslide material as an equivalent fluid. It is suitable to model the movement of materials with the property of fluid. Compared with the discrete numerical methods (Luo H et al., 2021; Zhuang Y et al., 2023b), the interaction between particles is ignored in the simulation. However, the continuum-based DAN3D model overcomes the high time cost of discrete numerical methods and can represent the essential processes of landslides, e.g., entrainment. Therefore, the DAN3D model is robust and effective for the landslide risk assessment. In the DAN3D model, the landslide dynamic is governed by the rheological relationships. The rheologies that have been found to provide great performances in simulating recorded events are frictional and Voellmy rheologies.

The frictional rheology regards the frictional resistance (τ) as a single-valued function of effective normal stress (σ):

$$\tau = \sigma(1 - r_u)\tan\varphi \tag{4}$$

where r_u represents the pore pressure ratio, and φ refers to the dynamic frictional angle.

The Voellmy rheology assumes that the combination of friction and turbulence governs the landslide motion:

$$\tau = \sigma f + \rho g v^2/\xi \tag{5}$$

where f represents the friction coefficient, ρ is the bulk density, and ξ refers to the turbulence parameter.

The entrainment is an important process during the landslide evolution. In the DAN3D model, A preliminary estimate of the average volume growth rate (E_s) for a specific entrainment area is obtained using the natural exponential growth equation (McDougall S and Hungr O, 2005):

$$V_f = V_0 \exp(E_s \cdot S) \quad (6)$$

where V_f is the estimated total volume of the landslide exiting the entrainment area, V_0 is the estimated total volume of the landslide entering the entrainment area, and S is the path length of the entrainment area. Using this equation, the average volume growth rate can be determined, which ensures that the required volume is entrained from the known length of the entrainment area.

In a DAN3D simulation, the required input data include the DEM of the landslide region and source area, rheological models and associated parameters. The DEMs can be easily obtained from a UAV survey or remote sensing, and the rheological parameters are determined through the back analysis until the simulated results highly agree with the actual situation.

During the back analysis of the numerical simulation, the multi-source data collaboration analysis results are used to help determine the rheological parameters. The simulated landslide velocity, duration and movement process are validated by the seismic signal analysis and video footage, and the simulated landslide deposit is validated by the ERT test results. The multi-source data collaboration analysis provides more information to check the modeling results and can thus provide reliable rheological parameters. These parameters can be directly used for the runout prediction of potential landslides that have a similar geological setting to recorded events. The overview framework for the landslide runout prediction is shown in Fig. 1.

3. Historical case analysis based on the multi-source data collaboration and numerical modeling

Southwest mountainous China is a landslide-prone region and massive landslide disasters have occurred in recent years (Yin YP et al., 2017; Fan XM et al., 2019). The region provides natural materials to research the dynamics of long runout landslides. This paper summarized our previous research on the Shuicheng landslide in the mountainous area in Guizhou, China, and performed the feasibility of

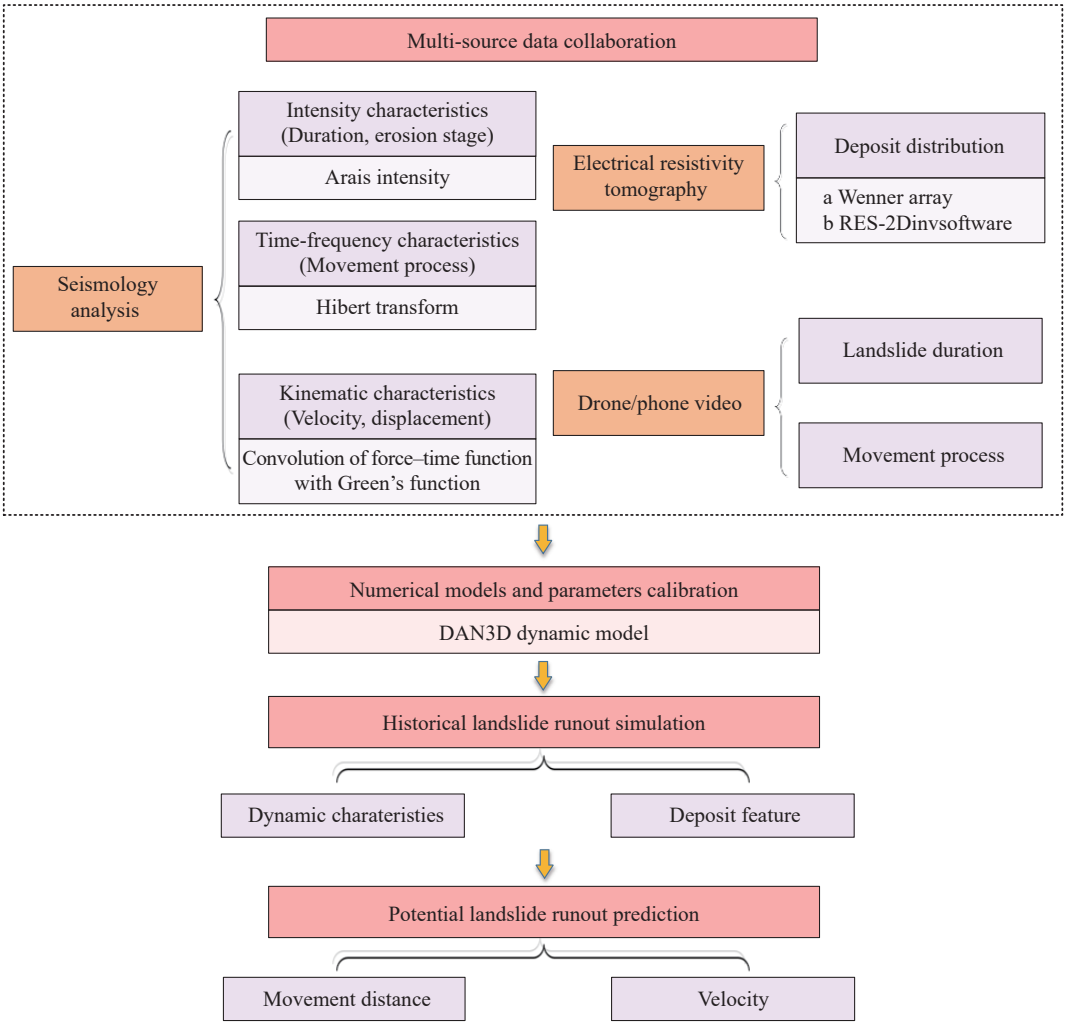

Fig. 1. Framework for the landslide runout prediction.

investigating landslide dynamics through multi-source data collaboration and numerical modeling. The landslide location is presented in Fig. 2a.

On 23th July 2017, a rainfall-triggered long runout landslide occurred in Shuicheng, Guizhou, China. The sliding mass moved 1250 m with an elevation difference of 465 m and caused 52 casualties (Fig. 2b). This disaster involved a total volume of about 2×10^6 m^3.

The Shuicheng landslide has an elevation ranging from 1180 m to 2270 m with an average slope angle of 24°. The source area has a steep topography of ~50° while the deposit area has a flat topography of 0°–10°. The exposed rocks in the study area range in age from Permian to Quaternary, and the landslide mainly occurred in the Emei Mountain basalt of Middle Permian (Zhang YB et al., 2020). The basalts in the source area are strongly weathered with fragmented cataclastic structures, and the materials in the travel path are primarily composed of Quaternary deposits (Zhuang Y et al., 2021). According to the local meteorological bureau, a cumulative rainfall of 189 mm happened within the 5 days before the event, leading to the Shuicheng landslide. The cataclastic structure of the weathered basalt made the released

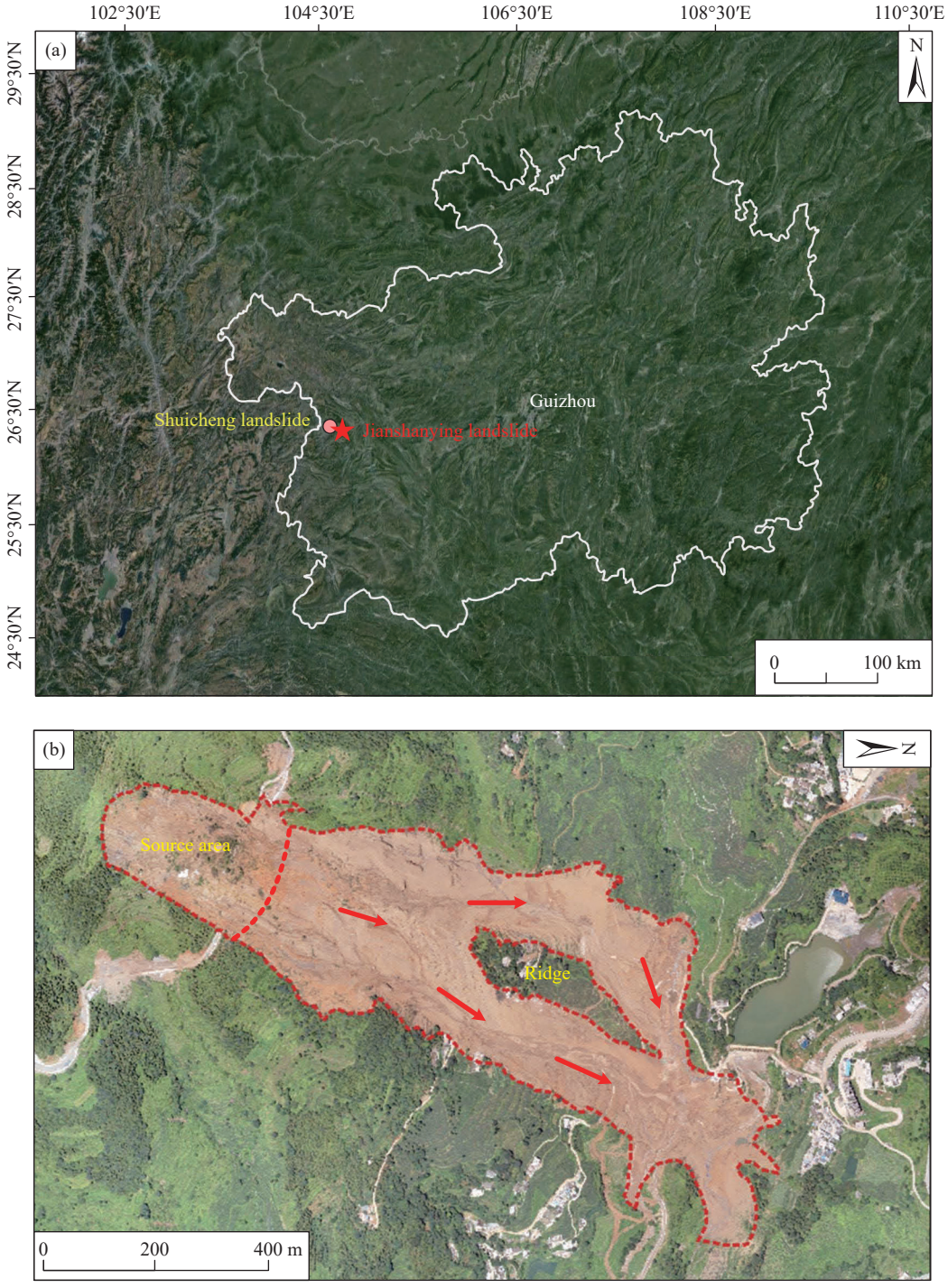

Fig. 2. (a) Locations of the landslide disasters in Guizhou, China. (b) Overview of the Shuicheng landslide.

rock mass transform into a debris avalanche shortly after the initiation, resulting in the long runout of the Shuicheng landslide.

The dynamic and deposit characteristics of the Shuicheng landslide were analyzed based on the combination of seismic signal, ERT survey and DAN3D modeling (Zhang YB et al., 2020; Zhuang Y et al., 2021;Fig. 3).

The landslide seismology analysis indicated that the Shuicheng landslide has a duration of about 60 s (Fig. 3a). In the initial stage (60–70 s), the sliding mass moved downward and accelerated because of the conversion of potential energy. Subsequently, the rapidly moving materials entrapped the loosed deposits and presented a complex movement path (70–108 s). Specifically, the sliding mass violently collided with the ridge, divided into two branches at about 80 s, and converged at the toe of the mountain at 95–100 s. In the final 12 s (108–120 s), the landslide movement was relatively slow and came to a stop at the deposit area. For the deposit features, 6 survey lines were installed in the landslide region. Two survey lines were in both gullies and two in the downstream deposit region. The inversed ERT images indicated the deposit depth of landslide profiles. In the surveyed profiles, the deposits show a depth distribution of 2–12 m, and the maximum value was identified in the downstream deposit region (Fig. 3f and g).

The multi-source data collaboration of seismic signal and ERT survey helped determine the rheological parameters (Table 1). The comparison results show high agreements in both landslide dynamics and deposit characteristics. The DAN3D simulated landslide dynamics at different time steps match the seismic signal well, including the duration, time steps of initiation, branching, and converging (Figs. 3a–e). The simulated deposit distribution is basically consistent with the ERT results.

Previous work on the Shuicheng long runout landslide (Zhang YB et al., 2020; Zhuang Y et al., 2021) confirmed the feasibility of determining rheological parameters for landslide modeling through multi-source data collaboration analysis. The multi-source data collaboration results provide valuable information about landslide characteristics and greatly improve the reliability of numerical parameters. It is suggested that the determined models and parameters can represent the essential process of landslide movement and help the prediction of potential landslides.

4. Runout prediction of the Jianshanying landslide

The Jianshanying mountain located in Shuicheng, Guizhou, China is one of the most dangerous landslide-prone regions in Guizhou. The authors have paid much attention to its risk assessment (Zhuang Y et al., 2021) and here the landslide that occurred on 16th September 2020 was selected to perform the runout prediction. This rainfall-triggered long runout landslide involves a volume of 8×10^5 m^3 and a travel distance of approximately 1 km. Fortunately, no people were killed in the event because of the timely warning and effective mitigation measures.

4.1. Geological and climate setting

The study area has an undulatory topography with strong cutting and belongs to the mountainous landform. An elevation difference of over 550 m is identified in the region, ranging from 1526 m at the top of Jianshanying mountain to 949 m at the outlet of Wanhe River (Dong JH et al., 2021). The pre-image of the Jianshanying mountain is presented in Fig. 4a.

The exposed strata in the study area from bottom to top are the Upper Permian Longtan Formation (P_3l), the Lower Triassic Feixianguan Formation (T_1f) and the Quaternary deposits (Q_4). The Upper Permian Longtan Formation is mainly composed of siltstone, mudstone, and coal seams, while the upper Feixianguan Formation consists of calcareous mudstone, sandstone, muddy siltstone and silty mudstone. Totally thirteen underground coal seams are identified in the region, and six of them have been mined. The long-term mining activities have greatly increased the slope deformation and frequently caused local rockslides, threatening the safety of 1062 residents.

The study area has a humid subtropical monsoon climate with an average annual temperature of around 15.8° (ranging from −6.3 °C to 32 °C). The annual rainfall is about 1027.2 mm, and is concentrated in the rainy season (from May to September). According to the rainfall monitoring equipment at the mountaintop, a cumulative rainfall of 184 mm from 12th July to 15th July was recorded (Fig. 5). The combined contribution of heavy rain and the long-term mining activities eventually initiated the landslide.

4.2. Jianshanying landslide

The Jianshanying landslide was initiated as a rock slide at the elevation of 1310 m. After detaching from the source area under the action of heavy rainfall, the sliding mass moved down in the north direction and disintegrated as a debris avalanche due to the violent impact with the slope surface. Subsequently, the rapidly moving materials entrained the loose deposits along the travel path, moved approximately 1 km, and finally stopped at Xiaozhai. This long runout landslide buried the Fanjiashaba, parts of houses in the Jiudianzi and Xiaozhai, destroyed 2 roads and caused mass economic loss and traffic paralysis. No people were killed in the event. With respect to its dynamics, the Jianshanying landslide is divided into two subzones: Source area (zone 1) and entrainment and deposit area (zone 2). The zone division and the longitudinal profile of the Jianshanying landslide are presented in Figs. 4 and 6.

The source area of the Jianshanying landslide ranges from 1250-1310 m, with an elevation difference of 60 m. Due to the long-term underground mining, massive cracks were developed in the area, providing preferential flow paths for rainfall infiltration. The joint impact of heavy rainfall and mining activities caused the failure of 8×10^5 m^3 materials and

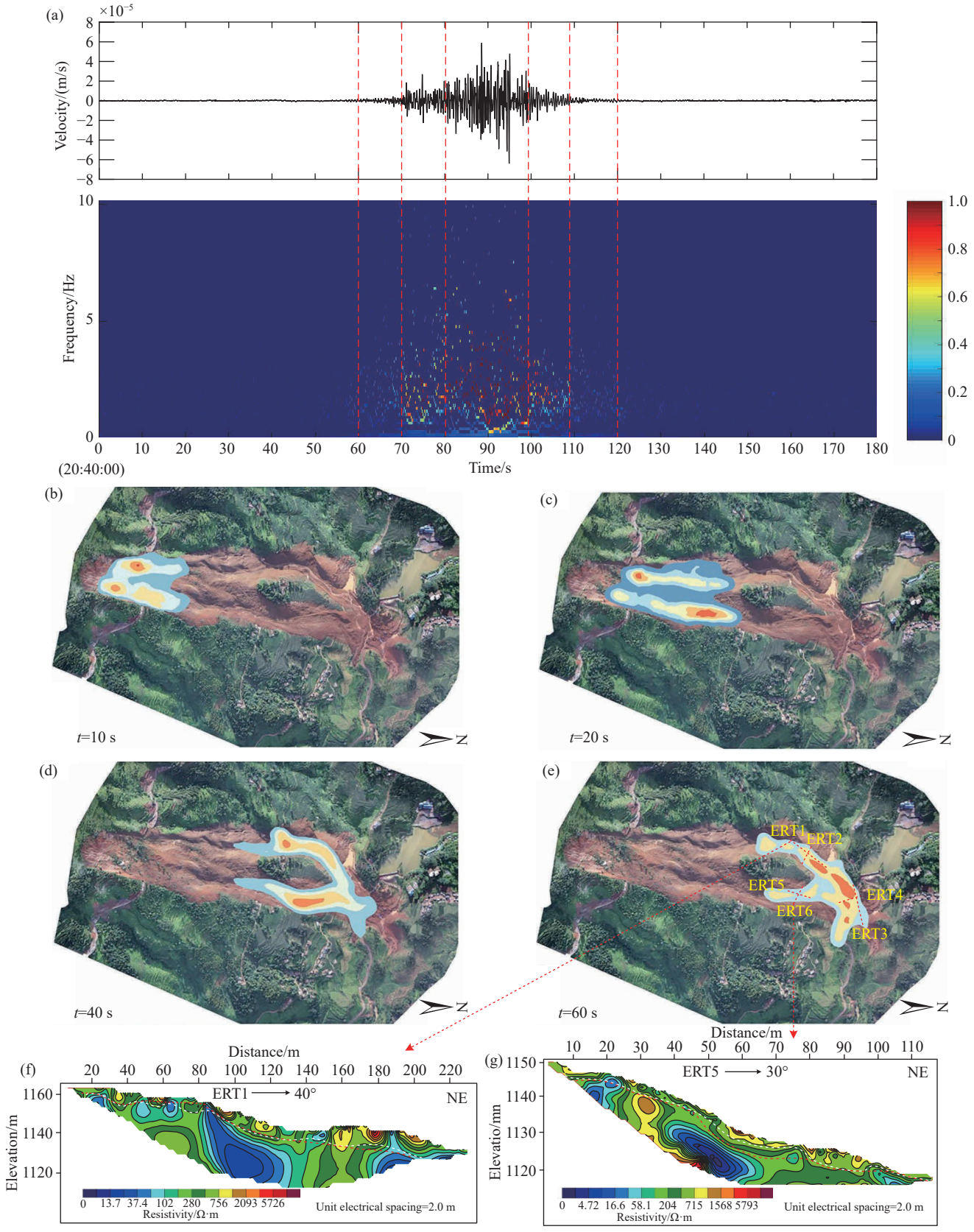

Fig. 3. Dynamic and deposit characteristics of the Shuicheng landslide (after Zhang YB et al., 2020 and Zhuang Y et al., 2021). a–Seismic signal analysis results; b–e–evolution process of the Shuicheng landslide simulated by DAN3D; f–g–ERT results testing the modeled landslide deposits. In the ERT inversion images, white dashed lines represent the hypothetical boundary from ERT results, and red dashed lines represent DAN3D simulated results.

resulted in this long runout landslide. The displaced rock mass in the source area is mainly strong weathered Feixianguan Formation of sandstone and mudstone.

The entrainment and deposit area is located at elevations

ranging from 1020 m to 1250 m, with a slope angle of 10°–50°. The zone has an average length of 800 m and a width of 420 m. A flat terrain was observed at the toe of mountain, and thus the sliding mass slowed down and stopped in the region.

The field investigation also focused on the cracks near the upper source area. These large cracks mainly resulted from the long-term creeping tensile action of the mountain and the unloading effect generated when the landslide occurred. The large cracks form a triangle-shaped potential landslide with an estimated volume of about 4×10^5 m^3, which dramatically threatens the downstream residents.

4.3. Landslide runout prediction of the 2020 Jianshanying landslide

The geological and geomorphological settings of the Jianshanying landslide and the Shuicheng landslide are in some terms similar. Both cases are located in Shuicheng county, showing a steep topography in the source area and a flat topography in the deposit area. The released materials are mainly composed of strong weathered rock mass, and the materials in the travel path are Quaternary deposits (Zhang YB et al., 2020). Heavy rainfall played a vital role in triggering these two landslides, and made the sliding mass and materials along the travel path highly saturated. The weathered rock mass in the source area transformed into the debris avalanche with high water content shortly after the initiation, finally leading to the long runout of both cases. When conducting landslide dynamic analysis with a depth-averaged model, the landslide movement is controlled by the rheology relationship, which is highly related to the characteristics of the sliding mass and the path materials. While the authors acknowledge the geological and geomorphological setting of the Shuicheng landslide and the Jianshanying landslide are not completely the same, the similar primary triggering factor (heavy rainfall),

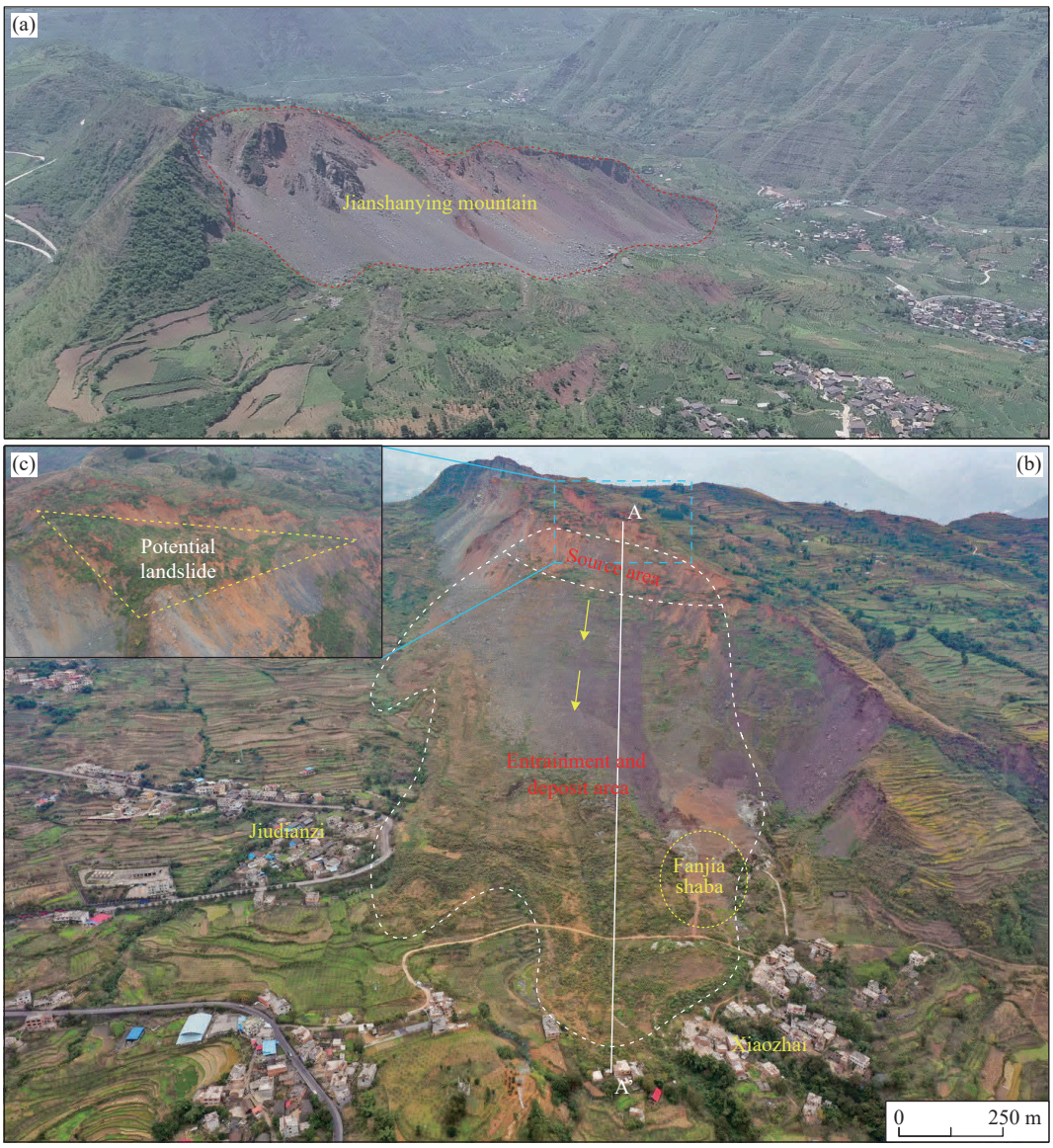

Fig. 4. View of the Jianshanying landslide. a–Jianshanying mountain in Shuicheng, Guizhou, China; b–shows the landslide region and zone division; c–the potential landslide at the top of mountain.

characteristics of the released (highly weathered, fragmented) and path materials (loose, saturated Quaternary deposits) caused the two landslides to have basically similar runout behaviors. Thus, the rheological parameters of the Shuicheng landslide are selected for the runout prediction of the Jianshanying landslide here (Table 1). Notably, the parameters used here are determined from the multi-source data collaboration analysis of the Shuicheng landslide, rather than the back analysis of the Jianshanying landslide.

Figs. 7–8 show the runout prediction results. The duration of the landslide motion is estimated at about 50 s with only internal deformation occurred in the following stage. The final deposit distribution of the sliding mass ranged from 0–12 m and was evenly distributed in the deposit region. In the initial 10 s, approximately 8×10^5 m^3 of sliding mass detached from the source area and moved along the north direction. The displaced materials then collided with the ridge at the elevation of 1160 m and few materials deflected to the direction of 25°. The main parts of sliding mass rapidly kept moving north and reached the Fanjiashanba and Jiudianzi at 30 s. The whole Fanjiashanba and parts of houses in the Jiudianzi were damaged in the stage. Subsequently, the landslide materials slowed down and stopped at the toe of the mountain at 50 s. Two roads were buried and a few houses in the Xiaozhai were damaged.

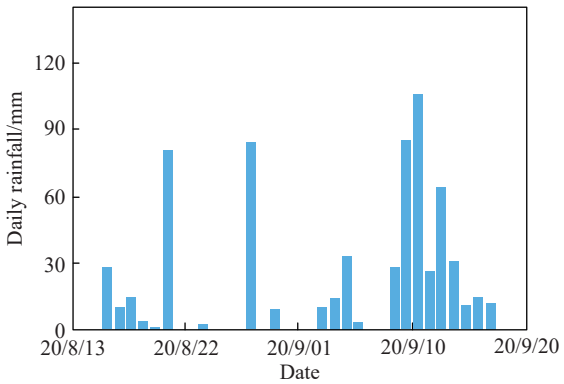

Fig. 5. Daily rainfall of the study area.

Fig. 8 shows the plot of maximum velocity versus runout distance. The maximum velocity of approximately 40 m/s was recorded at an elevation of 1190 m. The landslide region has a steep topography in the source area and a flat topography in the deposit area. Therefore, the sliding mass significantly accelerated in the initial stage and reached the maximum velocity in a short time. After entering the deposit area, the landslide mass started to spread in a fan shape and the velocity gradually decreased. At 50 s, the front margin of the sliding mass reached the Xiaozhai and stopped moving.

The landslide runout simulation based on the rheological parameters of the Shuicheng landslide had a great performance. The left leading edge of the landslide shows a slightly shorter distance, but overall, the landslide runout prediction results match the actual situation well. The simulation of the Jianshanying landslide confirmed the feasibility of the proposed runout prediction framework. The rheological parameters obtained from the multi-source data collaboration of historical landslide cases could greatly improve the accuracy of runout distance prediction.

4.4. Landslide runout prediction of the potential landslide

A potential landslide has been generated at the upper source area. As shown in Fig. 4c, the triangle-shaped potential source area is delineated by the large crack and involves an estimated volume of 4×10^5 m^3. This potential landslide has threatened the downstream residents and a landslide risk assessment is essential for disaster mitigation. Here, the landslide runout prediction is conducted based on the same rheological parameters as the 2020 Jianshanying landslide.

The DAN3D simulation results show that the potential landslide has a duration of about 60 s (Fig. 9). The potential landslide would slide down the surface of the existing landslide with a maximum movement distance of approximately 1 km. The sliding materials show a similar travel path with the existing landslide, except for a longer distance of the right branch that is divided at 1160 m (m.a.s.l.). The new deposit covers an area of approximately

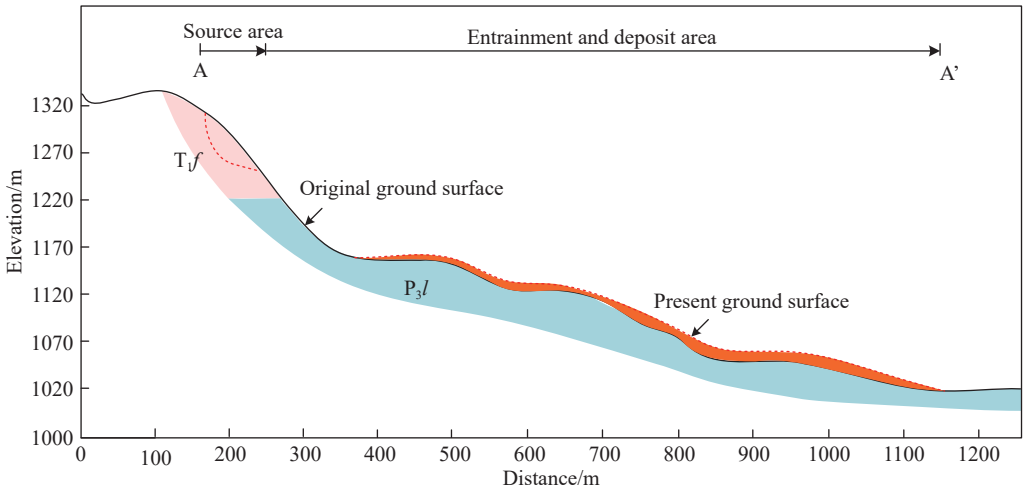

Fig. 6. Longitudinal profile of the Jianshanying landslide.

1.6×10^5 m^2 and its depth distribution ranges from 0 m to 8 m.

Based on the above results, the disaster scope of the potential landslide was plotted here (Fig. 10). The disaster scope shows a length of 585 m and a width of 455 m. Though most of the potential sliding mass deposits on the existing landslide, the right leading edge of the impact area exceeds the existing landslide boundary. Two roads and parts of houses in the Jiudianzi are still within the disaster scope of the potential landslide. Considering the constant deformation of the Jianshanying mountain and heavy rainfall in the rainy season, the downstream residents and the local traffic are threatened. The predictions can provide avoidance information for villages and help propose associated mitigation measures. Villages in dangerous areas should be evacuated promptly and warning signs need to be installed alongside the road.

This previous work on the historical case (Shuicheng landslides) and the runout prediction of the Jianshanying landslide demonstrated the feasibility of landslide dynamic analysis and runout prediction through the combination of multi-source data collaboration and numerical modelling. The multi-source data collaboration results provide valuable information to check the numerical results, which makes up for the deficiency of traditional back-analysis methods. The calibrated numerical parameters can help the runout prediction of landslides with a similar geological setting to the recorded events.

Table 1. Rheological models and parameters of the Shuicheng landslide.

Landslide	Zone	Rheology	φ(°)	r_u	f	ξ(m/s^2)
Shuicheng	Source	Frictional	24	0.4	–	–
	Entrainment and deposit	Voellmy	–	–	0.2	900

In recent years, the increased amount of available seismic stations has improved the opportunity to capture the seismic signals generated by large landslides (Schöpa A et al., 2018). The ERT method could image the landslide profiles with a rapid survey and relatively low cost (Samodra G et al., 2020). In addition, the entire landslide movement process can possibly be recorded using a mobile phone/drone when there are witnesses to the landslide initiation (Ma SY et al., 2019; Rapstine TD et al., 2020). These approaches make the multi-source data collaboration analysis easier, and the landslide information is no longer limited to field observations. Therefore, further case studies need to be performed based on the framework and a regional database of rheological parameters is recommended to be established. It is anticipated that the combination of multi-source data collaboration and numerical modeling could elevate the prediction accuracy of long runout landslides and help mitigate disasters in mountainous regions worldwide.

5. Conclusions

Long runout landslides have the characteristics of high mobility and powerful destructive power. They can cause

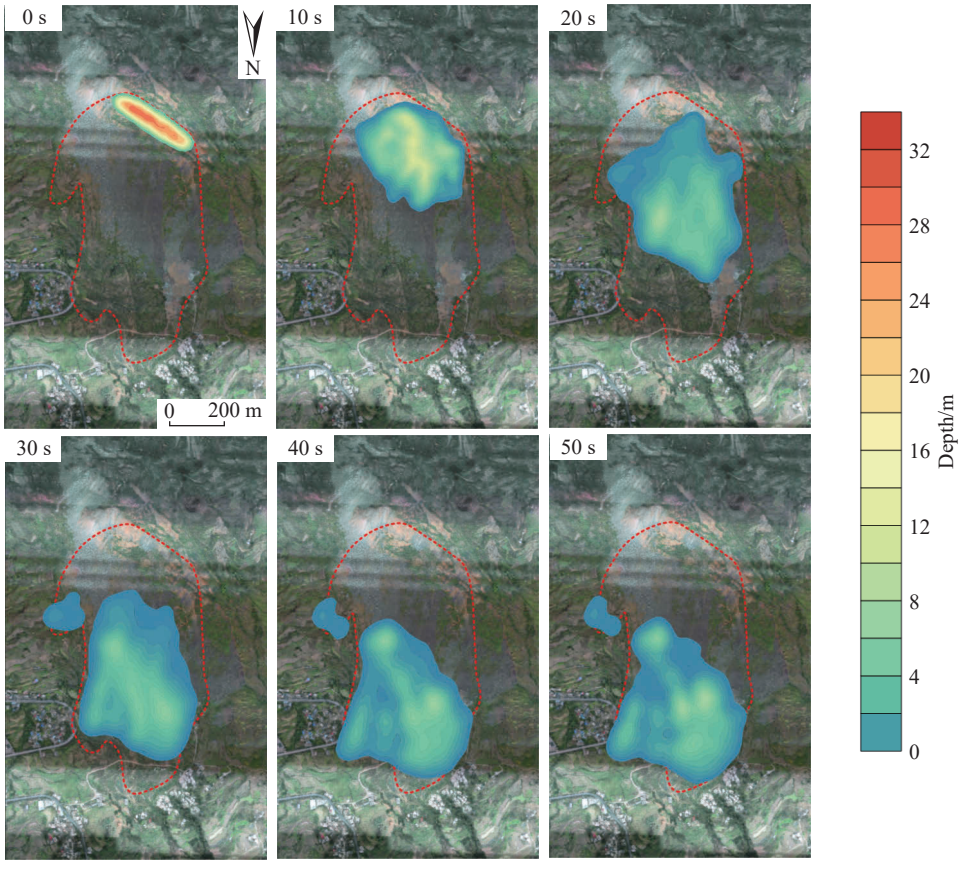

Fig. 7. Sliding process of the Jianshanying landslide simulated by Dan3D.

massive casualties and economic loss far from the source area. Predicting their runout is essential for risk assessment and disaster mitigation. This study proposed a framework for landslide runout prediction based on multi-source data collaboration and numerical modeling. The historical case of the Shuicheng landslide in Guizhou, China and the Jishanying landslide were analyzed to validate the proposed framework.

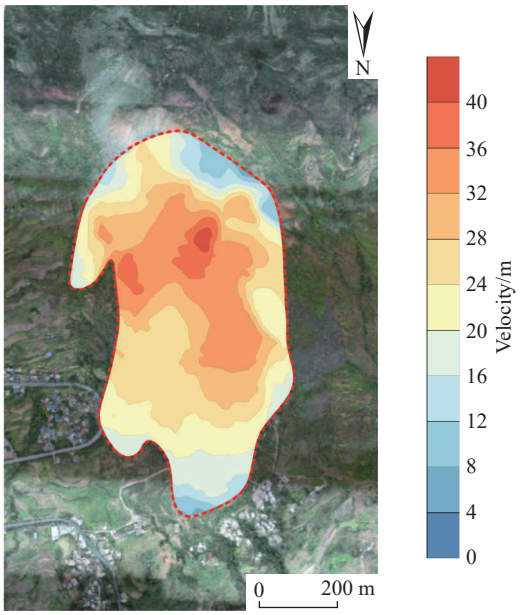

Fig. 8. Maximum velocity contour of the Jianshanying landslide.

This analysis of the Shuicheng landslide indicated that the multi-source collaboration analysis could validate the numerical results and help determine a group of convincing rheological parameters. The landslide seismology could provide information about landslide dynamics, while the ERT method could image the landslide profile to estimate the deposit distribution. The collaborated parameters can be used for the runout prediction of potential landslides with a similar geological setting to recorded cases. Furthermore, the Jianshanying landslide that occurred in 2020 was selected to perform the runout prediction. The selected rheological parameters are determined from the Shuicheng landslide, which has an adjacent location and similar geological settings to the Jianshanying landslide. Great comparison results were identified between the runout prediction and the actual situation, indicating the feasibility of the proposed framework for landslide runout prediction. Therefore, further case studies are recommended to be analyzed based on the combination of multi-source data collaboration and numerical modeling and a regional database of rheological parameters is worthwhile to be established. The work conducted in this study is expected to improve the prediction accuracy of landslide runout in the mountainous region worldwide.

CRediT authorship contribution statement

Ai-guo Xing and Yu Zhuang conceived of the presented idea. Jun Sun and Yu Zhuang carried out the field

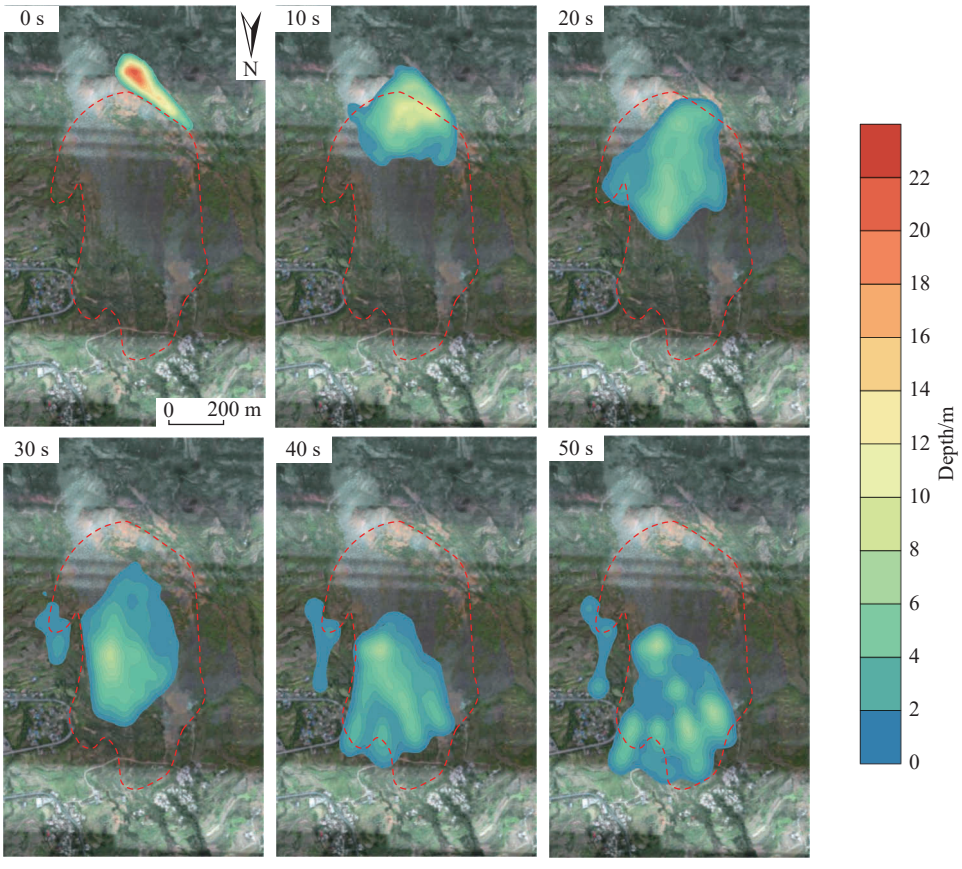

Fig. 9. Runout prediction of the potential landslide.

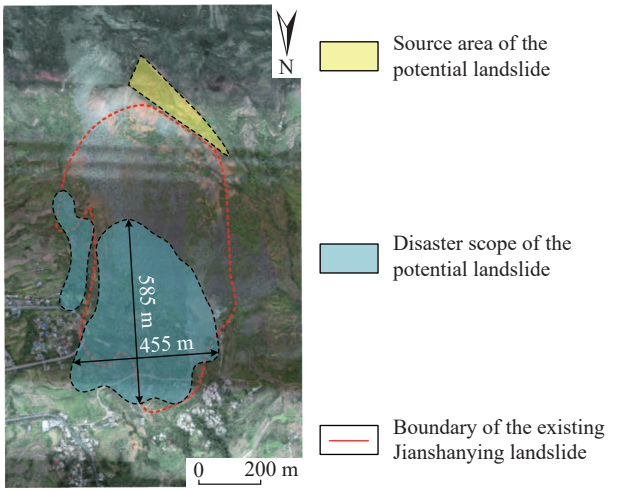

Fig. 10. Disaster scope of the potential landslide.

investigation. All authors discussed the results and contributed to the final manuscript.

Declaration of Competing Interest

The authors declare no conflicts of interest.

Acknowledgments

This study was supported by the National Natural Science Foundation of China (41977215).

References

Bellanova J, Calamita G, Giocoli A, Luongo R, Macchiato M, Perrone A, Uhlemann S, Piscitelli S. 2018. Electrical resistivity imaging for the characterization of the Montaguto landslide (southern Italy). Engineering Geology, 243, 272–281. doi: 10.1016/j.enggeo.2018.07.014.

Chen LQ, Zhao CY, Li B, He K, Ren CF, Liu XJ, Liu DL. 2021. Deformation monitoring and failure mode research of mining-induced Jianshanying landslide in karst mountain area, China with ALOS/PALSAR-2 images. Landslides, 18, 2739–2750. doi: 10.1007/s10346-021-01678-6.

Christen M, Kowalski J, Bartelt P. 2010. RAMMS: Numerical simulation of dense snow avalanches in three-dimensional terrain. Cold Regions Science and Technology, 63, 1–14. doi: 10.1016/j.coldregions.2010.04.005.

DEM Solutions Ltd. 2019. EDEM 2018 user guide, Edinburgh, UK.

Dong JH, Li HJ, Wang YS, Zhang YH. 2021. Characteristics and monitoring-based analysis on deformation mechanism of Jianshanying landslide, Guizhou Province, southwestern China. Arabian Journal of Geosciences, 14, 184. doi: 10.1007/s12517-021-08472-7.

Ekström G, Stark CP. 2013. Simple scaling of catastrophic landslide dynamics. Science, 339, 1416–1419. doi: 10.1126/science.123288.

Fan XM, Rossiter DG, Westen CJ, Xu Q, Görüm T. 2014. Empirical prediction of coseismic landslide dam formation. Earth Surface Process and Landforms, 39, 1913–1926. doi: 10.1002/esp.3585.

Fan XM, Xu Q, Liu J, Subramanian SS, He CY, Zhu X, Zhou L. 2019. Successful early warning and emergency response of a disastrous rockslide in Guizhou province, China. Landslides, 16, 2445–2457. doi: 10.1007/s10346-019-01269-6.

Frank F, McArdell BW, Huggel C, Vieli A. 2015. The importance of entrainment and bulking on debris flow runout modeling: examples from the Swiss Alps. Natural Hazards and Earth System Sciences 15, 2569–2583. doi:10.5194/nhess-15-2569-2015

Furman A, Ferré TPA, Warrick AW. 2003. A sensitivity analysis of electrical resistivity tomography array types using analytical element modeling. Vadose Zone Journal, 2, 416–423. doi: 10.2136/vzj2003.4160.

Geertsema M, Clague JJ, Schwab JW, Evans SG. 2006. An overview of recent large catastrophic landslides in northern British Columbia, Canada. Engineering Geology, 83, 120–143. doi: 10.1016/j.enggeo.2005.06.028.

He K, Chen C, Li B. 2018. Case study of a rockfall in Chongqing, China: movement characteristics of the initial failure process of a tower-shaped rock mass. Bulletin of Engineering Geology and the Environment, 78, 3295–3303. doi: 10.1007/s10064-018-1364-9.

Hibert C, Ekström G, Stark CP. 2014. Dynamics of the Bingham Canyon Mine landslides from seismic signal analysis. Geophysical Research Letters, 41, 4535–4541. doi: 10.1002/2014GL060592.

Hungr O, McDougall S, Bovis M. 2005. Entrainment of material by debris flows. In: Debris-flow Hazards and Related Phenomena. Springer Praxis Books. Springer, Berlin, Heidelberg.

Hungr O, McDougall S. 2009. Two numerical models for landslide dynamic analysis. Computers and Geosciences, 35(5), 978–992. doi: 10.1016/j.cageo.2007.12.003.

Hunter G, Fell R. 2003. Travel distance angle for “rapid” landslides in constructed and natural soil slopes. Canadian Geotechnical Journal, 40(6), 1123–1141. doi: 10.1139/t03-061.

Ishii Y, Ota K, Kuraoka S, Tsunaki R. 2012. Evaluation of slope stability by finite element method using observed displacement of landslide. Landslides, 9, 335–348. doi: 10.1007/s10346-011-0303-7.

Itasca Consulting Group Inc. 2008. PFC3D Particle Flow Code in 3 Dimensions, User’s Guide, Minneapolis.

Iverson RM, George DL, Allstadt K, Reid ME, Collins BD, Vallance JW, Schilling SP, Godt JW, Cannon CM, Magirl CS, Baum RL, Coe JA, Schulz WH, Bower JB. 2015. Landslide mobility and hazards: Implications of the 2014 Oso disaster. Earth and Planetary Science Letters, 412, 197–208. doi: 10.1016/j.epsl.2014.12.020.

Johnson BC, Campbell CS. 2017. Drop height and volume control the mobility of long-runout landslides on the Earth and Mars. Geophysical Research Letters, 44(12), 12091–12097. doi: 10.1002/2017GL076113.

Liu C, Pollard DD, Shi B. 2013. Analytical solutions and numerical tests of elastic and failure behaviors of close-packed lattice for brittle rocks and crystals. Journal of Geophysical Research: Solid Earth, 118(1), 71–82. doi: 10.1029/2012JB009615.

Luo H, Xing AG, Jin KP, Xu SM, Zhuang Y. 2021. Discrete element modeling of the Nayong rock avalanche, Guizhou, China Constrained by dynamic parameters from seismic signal inversion. Rock Mechanics and Rock Engineering, 54, 1629–1645. doi: 10.1007/s00603-021-02363-9.

Loke MH, Barker RD. 1996. Rapid least-squares inversion of apparent resistivity pseudo sections by a quasi-Newton method. Geophysical Prospecting, 44, 499–524. doi: 10.1111/j.1365-2478.1996.tb00142.x.

Ma SY, Xu C, Shao XY, Zhang PF, Liang XH, Tian YY. 2019. Geometric and kinematic features of a landslide in Mabian Sichuan, China, derived from UAV photography. Landslides, 16, 373–381. doi: 10.1007/s10346-018-1104-z.

Martorana R, Capizzi P, Alessandro A, Luzio D. 2017. Comparison of different sets of array configurations for multichannel 2D ERT acquisition. Journal of Applied Geophysics, 137, 34–48. doi: 10.1016/j.jappgeo.2016.12.012.

McCann DM, Forster A. 1990. Reconnaissance geophysical methods in landslide investigations. Engineering Geology, 29(1), 59–78. doi: 10.1016/0013-7952(90)90082-C.

McDougall S, Hungr O. 2005. Dynamic modelling of entrainment in rapid landslides. Canadian Geotechnical Journal, 42(5), 1437–1448. doi: 10.1139/t05-064.

Miao T, Liu ZY, Niu YH, Ma CW. 2001. A sliding block model for the runout prediction of high-speed landslides. Canadian Geotechnical Journal, 38, 217–226. doi: 10.1139/t00-092.

Morrison IM, Greenwood JR. 1989. Assumptions in simplified slope stability analysis by the method of slices. Géotechnique, 40(4), 655–658. doi: 10.1680/geot.1989.39.3.503.

Novellino A, Cesarano M, Cappelletti P, Martire DD, Napoli MD, Ramondini M, Sowter A, Calcaterra D. 2021. Slow-moving landslide risk assessment combining Machine Learning and InSAR techniques. Catena, 203, 105317. doi: 10.1016/j.catena.2021.105317.

Perrone A, Lapenna V, Piscitelli S. 2014. Electrical resistivity tomography technique for landslide investigation: A review. Earth-Science Reviews, 135, 65–82.

Rapstine TD, Rengers FK, Allstadt KE, Iverson RM, Smith JB, Obryk MK, Logan M, Oisen MJ. 2020. Reconstructing the velocity and deformation of a rapid Landslide using multiview video. Journal of Geophysical Research:Earth Surface, 125, e2019JF005348. doi: 10.1016/j.earscirev.2014.04.002.

Rezaei S, Shooshpasha I, Rezaei H. 2019. Reconstruction of landslide model from ERT, geotechnical, and field data, Nargeschal landslide, Iran. Bulletin of Engineering Geology and the Environment, 78(5), 3223–3237. doi: 10.1007/s10064-018-1352-0.

Samodra G, Ramadhan MF, Sartohadi J, Setiawan MA, Sukmawijaya S. 2020. Characterization of displacement and internal structure of landslides from multitemporal UAV and ERT imaging. Landslides, 17, 2455–2468. doi: 10.1007/s10346-020-01428-0.

Scheidegger AE. 1973. On the prediction of the reach and velocity of catastrophic landslides. Rock Mechanics, 5, 231–236. doi: 10.1007/BF01301796.

Schöpa A, Chao WA, Lipovsky BP, Hovius N, White RS, Green RG, Turowski JM. 2018. Dynamics of the Askja caldera July 2014 landslide, Iceland, from seismic signal analysis: precursor, motion and aftermath. Earth Surface Dynamics, 6, 467–485. doi: 10.5194/esurf-6-467-2018.

Sharma PS. 1997. Environmental and engineering geophysics. Cambridge University Press, 78–79.

Shi C, Zhang YL, Xu WY, Zhu QZ, Wang SN. 2013. Risk analysis of building damage induced by landslide impact disaster. European Journal of Environmental and Civil Engineering, 17(S1), 126–143. doi: 10.1080/19648189.2013.834590.

Stein S, Wysession M. 2003. An Introduction to Seismology, Earthquakes, and Earth Structure. John Wiley & Sons.

Strom A. 2006. Morphology and internal structure of rockslides and rock avalanches: grounds and constraints for their modeling. In: Evans SG, Mugnossa GS, Strom A, Hermanns RL. (Eds.), Landslides From Massive Rock Slope Failure, NATO Sciences Series, IV. Earth and Environmental Sciences, 49, 305–326. doi: 10.1007/978-1-4020-4037-5_17

Szczygieł J, Mendeck, M, Hercman H, Wroblewski W, Glazer M. 2019. Relict landslide development as inferred from speleothem deformation, tectonic data, and geoelectrics. Geomorphology, 330, 1160–128. doi: 10.1016/j.geomorph.2019.01.017.

Thompson N, Bennett MR, Perfort N. 2009. Analyses on granular mass movement mechanics and deformationwith distinct element numerical modeling: implicationsfor large-scale rock and debris avalanches. Acta Geotechnica, 4, 233–247. doi: 10.1007/s11440-009-0093-4.

Tomás R, Abellán A, Cano M, Riquelme A, Tenza-Abril AJ, Baeza-Brotons F, Saval JM, Jaboyedoff M. 2017. A multidisciplinary approach for the investigation of a rock spreading on an urban slope. Landslides, 15, 199–207. doi: 10.1007/s10346-017-0865-0.

Xu L, Dai FC, Tham LG, Zhou YF, Wu CX. 2012. Investigating landslide-related cracks along the edge of two loess platforms in northwest China. Earth Surface Processes and Landforms, 37(10), 1023–1033. doi: 10.1002/esp.3214.

Yalcinkaya E, Alp H, Ozei O, Gorgun E, Martino S, Lenti L, Bourdeau C, Bigarre P, Coccia S. 2016. Near-surface geophysical methods for investigating the Buyukcekmece landslide in Istanbul, Turkey. Journal of Applied Geophysics, 134, 23–35. doi:10.1016/j.jappgeo.2016.08.012

Yin YP, Xing AG, Wang G, Feng Z, Li B, Jiang Y. 2017. Experimental and numerical investigations of a catastrophic long-runout landslide in Zhenxiong, Yunnan, southwestern China. Landslides, 14, 649–659. doi: 10.1007/s10346-016-0729-z.

Zhang YB, Xing AG, Jin KP, Zhuang Y, Bilal M, Xu SM, Zhu YQ. 2020. Investigation and dynamic analyses of rockslide-induced debris avalanche in Shuicheng, Guizhou, China. Landslides, 17, 2189–2203. doi: 10.1007/s10346-020-01436-0.

Zhu YQ, Xu SM, Zhuang Y, Dai XJ, Lv G, Xing AG. 2019. Characteristics and runout behaviour of the disastrous 28 August 2017 rock avalanche in Nayong, Guizhou, China. Engineering Geology, 259, 105154. doi: 10.1016/j.enggeo.2019.105154.

Zhuang Y, Xing AG, Cheng QG, Li DS, Zhao C, Xu C. 2019. Characteristics and numerical modeling of a catastrophic loess flow slide triggered by the 2013 Minxian–Zhangxian earthquake in Yongguang village, Minxian, Gansu, China. Bulletin of Engineering Geology and the Environment, 79, 439–449. doi: 10.1007/s10064-019-01542-x.

Zhuang Y, Xing AG, Leng YY, Bilal M, Zhang YB, Jin KP, He JY. 2021. Investigation of Characteristics of Long Runout Landslides Based on the multi-source Data Collaboration: A Case Study of the Shuicheng Basalt Landslide in Guizhou, China. Rock Mechanics and Rock Engineering, 54, 3783–3798. doi: 10.1007/s00603-021-02493-0.

Zhuang Y, Xing, AG, Jiang YH, Sun Q, Yan JK, Zhang YB. 2022. Typhoon, rainfall and trees jointly cause landslides in coastal regions. Engineering Geology, 298, 106561. doi: 10.1016/j.enggeo.2022.106561.

Zhuang Y, Piazza N, Xing AG, Christen M, Bebi P, Bottero A, Stoffel L, Glaus J, Bartelt P. 2023a. Tree blow-down by snow avalanche air-blasts: Dynamic magnification effects and turbulence. Geophysical Research Letters, 50, e2023GL105334. doi: 10.1029/2023GL105334.

Zhuang Y, Xu Q, Xing AG, Bilal M, Gnyawali KR. 2023b. Catastrophic air blasts triggered by large ice/rock avalanches. Landslides, 20, 53–64. doi: 10.1007/s10346-022-01967-8.